Determining the Direct Capture Rate of $^{11}C(p, ()^{12}N$ with the $^{14}N(^{11}C, ^{12}N)^{13}C$ Reaction

X. Tang, A. Azhari, V. Burjan[a], F. Carstoiu[b], C. A. Gagliardi, V. Kroha, A. M. Mukhamedzhanov, A. Sattarov[c], L. Trache and R. E. Tribble

[a]*Institute of Nuclear Physics, Czech Academy of Sciences, Czech Republic*

[b]*Institute of Physics and Nuclear Physics, Romania*

[c]*Department of Physics, Texas A&M University, Texas 77843, USA*

In order to obtain a new determination of the direct capture reaction rate for $^{11}C(p, ()^{12}N$ at astrophysical energies[l] [2], the asymptotic normalization coefficient, ANC, for $^{12}N \leftrightarrow p + ^{11}C$ was extracted from the peripheral proton transfer reaction ^{14}N (^{11}C, $^{12}N)^{13}C_{g.s.}$, which was performed at the Cyclotron Institute using a ^{11}C radioactive beam. Background information and the details about the experimental procedure can be found in previous reports[3]. We focus here on the analysis and results.

Reaction channels were identified using the Particle ID (PID) Vs Q value (Qval) spectrum shown in Fig. 1. The Q value was calculated with the assumption of ^{11}C elastic scattering on ^{14}N. Due to a thickness variation of the)E detector the PID varied at different locations. So we divided the telescope into a 16 x 16 grid. The PID of every event was normalized to the average ^{11}C PID according to the grid. Then the elastic and primary transfer channels are clearly separated from the other reaction products.

The elastic scattering angular distribution was predicted using two sets of renormalized optical model parameters obtained from double folding Hartree-Fock density distributions with the JLM effective interaction [4]. One set is for loosely bound systems and the other is for tightly bound. Due

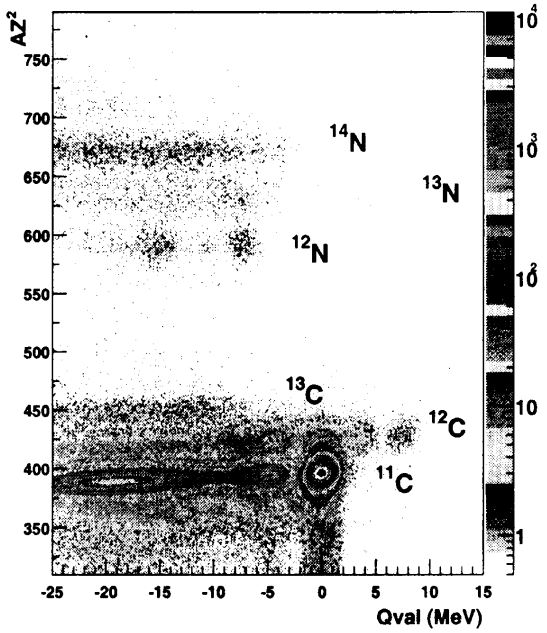

Figure 1: A typical particle identification (PID) vs. Q value (Qval) for different reaction channels. The ^{11}C group with Qval around 0 MeV is the elastic channel and the least negative Q-value peak in ^{12}N is from ^{14}N (^{11}C, $^{12}N)^{13}C$***g.s.***.

to factors like energy spread, angular divergence and position shift of the beam, and finite resolution of the detectors, the predicted angular distribution is smeared. A detailed Monte Carlo simulation program, which considered all the information about the beam and detectors, was employed to generate the predicted angular distributions after smearing was applied. The elastic scattering of ^{11}C on melamine was identified by PID and Qval. The

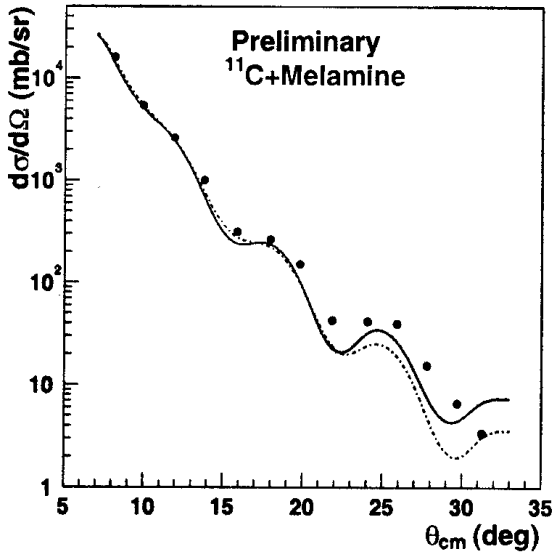

Figure 2: Elastic angular distributions for ^{11}C on melamine. Two sets of predicted distributions are shown. The solid curve used the parameters for tightly bound nuclei while the dashed curve used those for loosely bound nuclei.

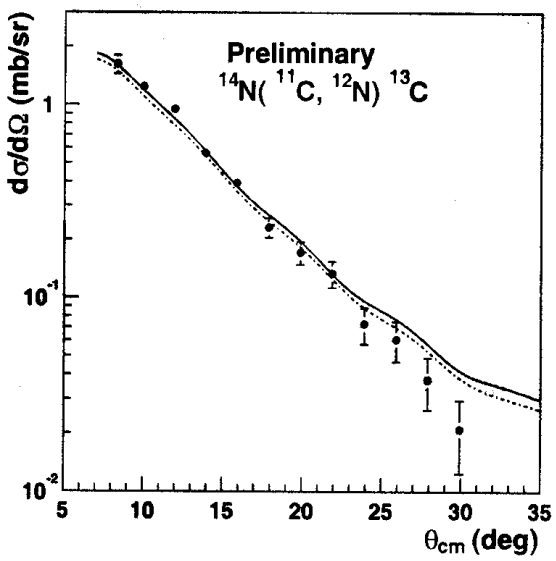

Figure 3: Transfer angular distributions for 14 N(^{11}C,^{12} N) $^{13}C_{g.s.}$. Two sets of predicted distributions are shown. The dashed curve used the parameters for loosely bound nuclei for both the incoming and outgoing channel. The solid used the parameters for the tightly bound nuclei for the incoming channel and those for loosely bound for the outgoing channel.

result is shown in Fig. 2 together with tightly bound (solid) and loosely bound (dash) calculations. The tightly bound calculation gives a better fit for the experimental data at large angles because ^{11}C is a rather stable nucleus. Since we can not distinguish $^{11}C + ^{11}C$ elastic scattering from $^{11}C + ^{14}N$, the elastic angular distributions shown are the sum of the two elastic scattering channels in the target according to their atomic ratio.

The proton transfer reaction ^{14}N (^{11}C, ^{12}N)$^{13}C_{g.s.}$ also was identified by PID and Qval. The angular distribution is shown in Fig. 3 together with the two sets of predictions. The solid curve is a DWBA prediction that used the tightly bound optical model parameters for the incoming channel and loosely bound optical model parameters for the outgoing channel. The dashed curve in Fig. 3 is a DWBA calculation that used loosely bound optical parameters for both incoming and outgoing channels. It demonstrates that the sensitivity to the choice of the double-folding potential renormalization factors illustrated in Fig. 2 leads to an uncertainty in the inferred ANC of only 4%. In the DWBA calculations, the ratios of $p_{3/2}$:$p_{1/2}$ was kept at 0.24 which was obtained from shell model calculations[5]. The value of the ANC's for $^{12}N \leftrightarrow p + ^{11}C$ were found to be $C^1_{1/2} = 1.4 \pm 0.2 \pm 0.08\, fm^{-1}$ and $C^2_{3/2} = 0.33 \pm 0.05 \pm 0.08\, fm^{-1}$. The contributions to the first uncertainty are: statistics (3.0%), absolute normalization of the measured cross section (5.0%), inputs to the Monte Carlo simulation (2.0%), inputs to the DWBA (10.0%), and knowledge of the $^{14}N \leftrightarrow p + ^{13}C$ ANC (6.4%). The second uncertainty is estimated by varying the ratio Of $p_{3/2}$:$p_{1/2}$ in a range of 20% which makes a 9.1% error for the astrophysical S factor. The lower limit for the Γ_{γ}, width of the second resonance

of ^{12}N was re-estimated to be 42 meV, which is close to the result of a GCM calculation[6], using an R-Matrix approach with the new ANC's.

With the new ANC's, the S factor for ^{11}C(p,()^{12}N was updated and the result is shown in Fig. 4 together with the GANIL result [7]. The upper solid lines show our updated S factors. The lower solid line for direct capture is larger and more precise than the GANIL result. With our results, the first resonance stays the same while the second resonance is larger by a factor of about 7. The low energy S factor is greatly enhanced by the interference between the direct capture and the second resonance. The new reaction rate is shown in Fig. 5. For T_9 between 0.2 and 0.4, the new reaction rate is 2 times larger than the old rate. As a result, the proposed rap II and III processes [2] will occur at lower density.

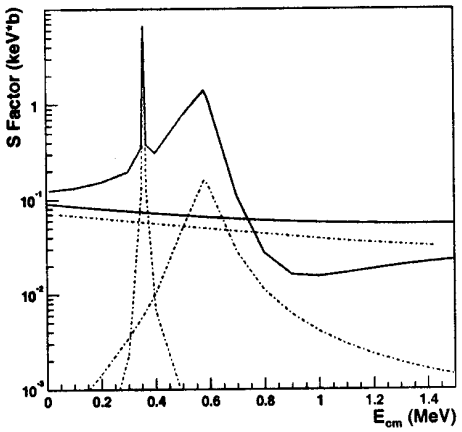

Figure 4: S factor for ^{11}C(p, ()^{12}N. The solid lines are our results and the dashed are the GANIL results.

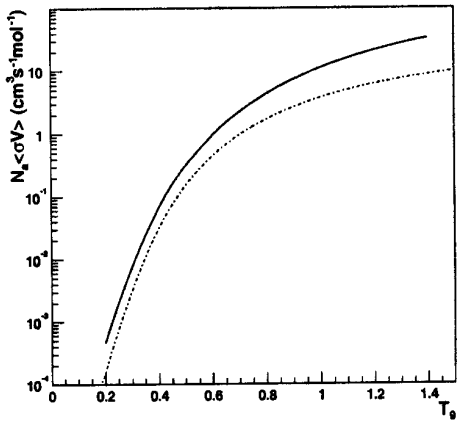

Figure 5: Reaction rate for ^{11}C(p, ()^{12}N. The solid line is our result and the dashed is the GANIL result.

References

[1] G. Fuller *et al*., Ap. J. **307,** 675 (1986).

[2] M. Wiescher *et al*., Ap. J. **343,** 352 (1989).

[3] X. Tang *et al*., *Progress in Research*, Cyclotron Institute, Texas A&M University (1999-2000), PI-8.

[4] L. Trache *et al*., Phys. Rev. C **61,** 024612-1 (2000).

[5] S. Cohen and D. Kurath, Nucl. Phys. **A101,** (1967).

[6] P. Descouvemont, Nucl. Phys. **A646,** 21 (1999).

[7] A. Leebvre *et al*., Nucl. Phys. **A592,** 69 (1995).